# A Parallel Wire Robot for Epicardial Interventions

Adam D. Costanza, Nathan A. Wood, Michael J. Passineau, Robert J. Moraca, Stephen H. Bailey, Tomo Yoshizumi, and Cameron N. Riviere

***Abstract*—This paper describes the design and preliminary testing of a planar parallel wire robot that adheres to the surface of the beating heart and provides a stable platform for minimally invasive epicardial therapies. The device is deployed through a small subxiphoid skin incision and attaches to the heart using suction. This methodology obviates mechanical stabilization and lung deflation, which are typically required during minimally invasive beating-heart surgery. The prototype design involves three vacuum chambers connected by two flexible arms. The chambers adhere to the epicardium, forming the vertices of a triangular base structure. Three cables connect a movable end-effector head to the three bases; the cables then pass out of the body to external actuators. The surgical tool moves within the triangular workspace to perform injections, ablation, or other tasks on the beating heart. Tests *in vitro* and *in vivo* were conducted to demonstrate the capabilities of the system. Tests *in vivo* successfully demonstrated the ability to deploy through a subxiphoid incision, adhere to the surface of the beating heart, move the surgical tool head within the robot's workspace, and perform injections into the myocardium.**

## I. Introduction

Multiple promising gene therapies for heart failure are currently under development [1], [2], but they lack effective means for delivery to the myocardium [3]. Homogeneity of gene expression is important in order to avoid arrhythmia [4]; therefore, a large number of small injections is needed over a relatively large area. This large number of injections must be placed accurately, and preferably while the heart is beating, in order to avoid the morbidity associated with cardiopulmonary bypass [5].

Minimally invasive methods for cardiac interventions possess significant advantages to standard open procedures including decreasing both the risk of infection and recovery times for patients [6]. Thoracoscopy is frequently used as a means to access the heart in a minimally invasive manner [7]. While thoracoscopic techniques are preferable to open heart surgery, they are still traumatic in that the lung must be deflated in order to gain access to the heart. In addition, the rigidity of the tools limits access to a small portion of the heart. Another limiting factor in thoracic procedures is the periodic motion of the beating heart. Stabilization devices are required to enable interventions on the beating heart.

The device introduced in this work overcomes these limitations in two ways. The device is delivered to the heart using a subxiphoid approach, obviating lung deflation. Once delivered to the pericardial space, the device adheres to the surface using vacuum pressure, providing a platform of zero relative motion with the beating heart. With the device, not only is the surgery less invasive, but it can also access parts of the heart unreachable by thoracoscopic tools.

The device is a parallel wire robot, shown in Fig. 1. It is different from conventional surgical manipulators in that it adheres to the heart, providing a stable platform to deliver treatments, in a manner similar to the epicardial crawling robot known as HeartLander [8]. The present device is somewhat more complicated than HeartLander, but as a parallel wire robot, it can access a larger workspace considerably more rapidly [9]. Because the proposed device is affixed to the heart, injections can be placed more accurately despite the heartbeat; because it is a parallel wire robot, it can rapidly cover the target area.

Currently, da Vinci® is the only commercially available robot that can be used in cardiothoracic surgeries [10]. However, it has difficulty both in accurately intervening on the beating heart, and in accessing large areas of the surface [11]. To date, there is no commercially available cardiac robot for reliable and accurate performance of injections into the heart.

Parallel wire robots have been a subject of research since the 1980's [9]. One of the first well-known wire robots was the NIST ROBOCRANE [12]. Parallel wire robots

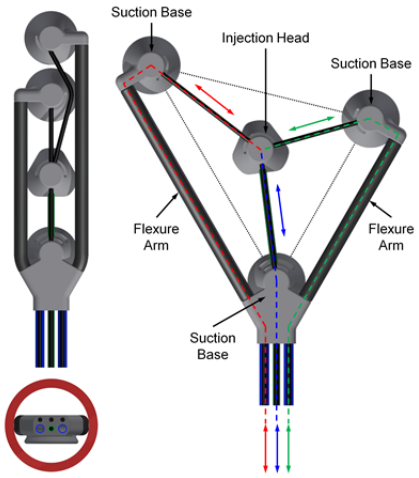


Fig. 1. Epicardial wire robot for rapid accurate myocardial injection for gene therapy. (a) The manipulator collapses for endoscopic insertion and removal. (b) After insertion, it deploys in triangular shape, with its three corners grasping the epicardium with suction. By pulling the 3 cables that connect the injection head to the 3 suction bases, injections can be rapidly and accurately placed anywhere within the dotted triangle.

This work was supported in part by the Disruptive Health Technology Institute at Carnegie Mellon University, the Semiconductor Research Corporation, and the U.S. National Institutes of Health (grant nos. R01HL078839 and R01HL105911).

A. D. Costanza, N. A. Wood, and C. N. Riviere are with the Robotics Institute, Carnegie Mellon University, Pittsburgh PA 15213, USA (email: camr@ri.cmu.edu).

M. J. Passineau is with the Division of Cardiovascular Medicine, Allegheny General Hospital, Pittsburgh, PA 15212, USA.

R. J. Moraca and S. H. Bailey are with the Dept. of Thoracic and Cardiovascular Surgery, Allegheny Gen. Hosp., Pittsburgh, PA 15212, USA.

T. Yoshizumi is with the McGowan Institute of Regenerative Medicine, Pittsburgh, PA 15219, USA.

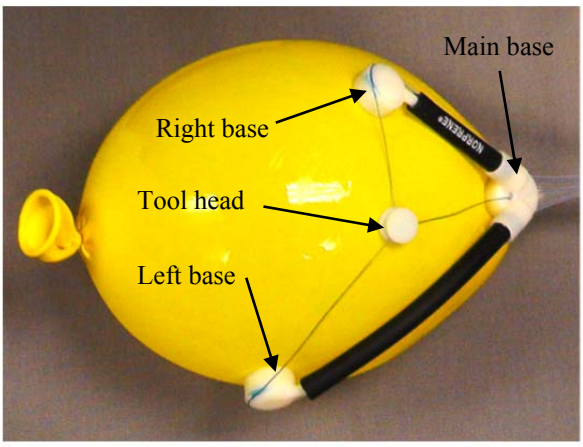


Fig. 2 Epicardial parallel wire robot deployed onto a balloon. By pulling the three wires using external actuators, the tool head can be positioned anywhere within the triangular workspace.

overcome the limitations on workspace in classical parallel robots by replacing linear actuators with cables. This allows for larger workspaces, higher speeds and accelerations, and lower moving masses [13]. The system proposed here can be defined as a planar wire robot with one degree of actuation redundancy [14] if the curvature of the heart surface is neglected. As such, statics and kinematics can be determined using previously developed methods [14].

## II. Methods

### A. Device Design

The prototype epicardial wire robot is shown in Fig. 2. The device consists of the two distal suction bases and a proximal suction base built using rapid prototyping techniques. The two arms connecting the left and right distal bases to the proximal base are made of neoprene tube, through which Tygon™ suction lines and PTFE sheaths for the drive cables are delivered to the distal bases.

This prototype relies on the compliance of the arms to allow the device to passively fold to fit within the delivery cannula, and, upon exiting, to return to the deployed state. The compliance in the arms also allows the device to attach to a curved surface at the three base locations. The position of the injection head can be adjusted by pulling on the three drive wires which run from the head to each base, through the PTFE sheaths in the flexure arms, and out of the proximal base. The drive wires in the current prototype consist of braided fishing line. The longer arm is 100 mm long, and the shorter arm 75 mm.

### B. Kinematics

For motion and path planning a planar approximation has been made. Because the device is a parallel manipulator, no closed form solution exists for the forward kinematics. However, the planar approximation means that the inverse kinematics can be solved by drawing a circle concentric to each base and finding the radius of each circle when they all intersect at the same point, as shown in Fig. 3. This represents the Euclidean distance between the points [15].

From this, planning algorithms have been developed that will allow surgeons to draw a path or a series of injection

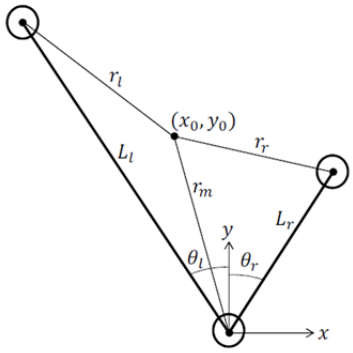


Fig. 3. Ideal kinematics of the planar wire robot manipulator.

sites, to which the manipulator can autonomously travel under minimum-jerk trajectory conditions. The inverse kinematics means that by using the robot Jacobian, the Cartesian coordinate space can be directly translated into the coordinate space of the robot [14]. The geometry of the device yields the inverse kinematics:

$$\begin{bmatrix} r_l \\ r_r \\ r_m \end{bmatrix}^2 = \begin{bmatrix} [x_0+L_l\cos(\theta_l)]^2+[y_0-L_l\sin(\theta_l)]^2 \\ [x_0-L_r\cos(\theta_r)]^2+[y_0-L_r\sin(\theta_r)]^2 \\ {x_0}^2+{y_0}^2 \end{bmatrix} \quad (1)$$

### C. Cardiac Access

The device is designed to access the heart in a minimally invasive way by utilizing a subxiphoid approach. After subxiphoid access is created and an incision is made in the pericardium, the manipulator is inserted into a 20-mm cannula. This cannula is inserted into the hole, and by pushing on the back end of the manipulator, it is deployed onto the heart under the pericardium. The stiffness of the arms allows the robot to passively open on the heart, obviating onboard motors or springs.

Once deployed onto the heart, suction is turned on to secure the manipulator to the heart. The tether for the injection head slides freely in the main base, allowing the surgical tool to be moved rapidly anywhere within the workspace. Injection is performed manually.

### D. Electronic Control System

In order to provide precise and accurate control of the tool, an electronic control system has been developed. A side view of the system can be seen in Fig. 4. The low-level control system includes an Arduino Mega 2560 microcontroller, three continuous-rotation servos, and three encoders for position feedback.

Control is performed using only position feedback as the output and servo speed as the input. Three independent PID loops run at 1000 Hz. The PID controllers were independently tuned by first estimating a transfer function numerically using MATLAB's System Identification Toolbox and then using the function *pidtune* to tune for a unit step function input. The control system has a graphical user interface (GUI) that allows the surgeon to control the device remotely.

### E. Geometric Homing

Due to the flexibility of the arms, the deployed geometry of the device can vary due to the unpredictable operating

environment. In order to account for this, geometric homing is done using the encoders which measure differential wire length. In the homing procedure, the tool head is moved manually to each base, in sequence. By calculating the difference in encoder values, the changes in cable lengths are determined, allowing for recovery of the deployed device geometry.

## III. Results

Movement of the injection head, suction, and injection have been tested *in vitro*. The device was first tested on a balloon coated in lubricant with a stocking pulled over it to simulate the heart and pericardium. Prototypes that demonstrated successful suction and movement of the injector head were then tested for injection into animal muscle tissue *ex vivo*. In all, 16 prototypes were tested.

The manipulator was then tested *in vivo* in a porcine model ($N = 3$) under a board-approved protocol. The device was inserted using subxiphoid access and tested for movement of the injection head, injection of ink, suction, and visualization under fluoroscope.

### A. *Testing* in vitro

No prototypes had difficulty adhering to the balloon or chicken breast during testing *in vitro*. Initial difficulties were overcome in movement of the injection head. Rotation of the tether sometimes caused the head to rotate as well. Redesign to relocate the anchor positions for the strings allowed for the rotational moment to be minimized. Ink injection into the chicken tissue was performed and deemed successful at a depth of 5 mm.

### B. *Geometric Homing*

Benchtop tests were conducted to ensure that the previously described geometric homing procedure provided accurate results. Because two measurements are made for each string length (i.e., as one string shortens, another lengthens when going from one base to another), comparing the two measurements allowed verification. Measurements within 5% of each other were considered accurate.

Use of these measurements quantifies the size of the robot, and then rotation of the axes is chosen, as seen in Fig. 3, letting $\theta_l = \theta_r$ to simplify calculations. During tabletop testing, the length of the left and right sides of the workspace were measured via geometric homing as 80.1 mm and 61.9 mm respectively, while the actual dimensions were 83 mm and 62 mm, corresponding to errors of 3.5% and 0.2%, respectively.

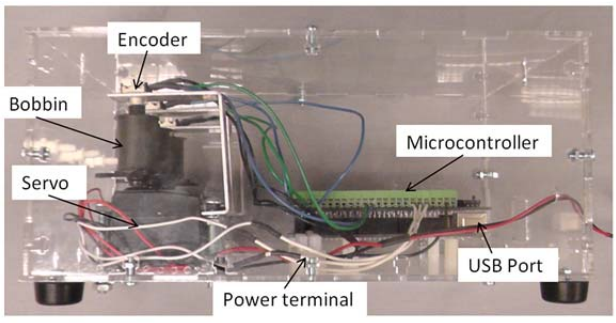


Fig. 4. Control system in acrylic box. Each servo rotates a bobbin that tensions the corresponding cable of the manipulator.

(a) (b)

Fig. 5. (a) Manipulator in cannula before insertion. (b) Manipulator deployed *in vivo* via subxiphoid access.

### C. *Testing* in vivo

#### 1) *Insertion and Deployment*

The manipulator was successfully inserted and deployed via subxiphoid access and a small incision in the pericardium near the apex of the heart. Images from before and after the insertion are shown in Fig. 5. During insertion the device was collapsed inside the cannula, and the cannula was inserted into the pericardial space. The device was advanced through the cannula to the heart surface. As the device exited the cannula, the flexible arms expanded to the deployed state and suction was provided to the bases to adhere to the surface of the heart. In some cases, because there is some error in the positioning of the wires, twisting can occur under deployment. This means the wires will cause forces that

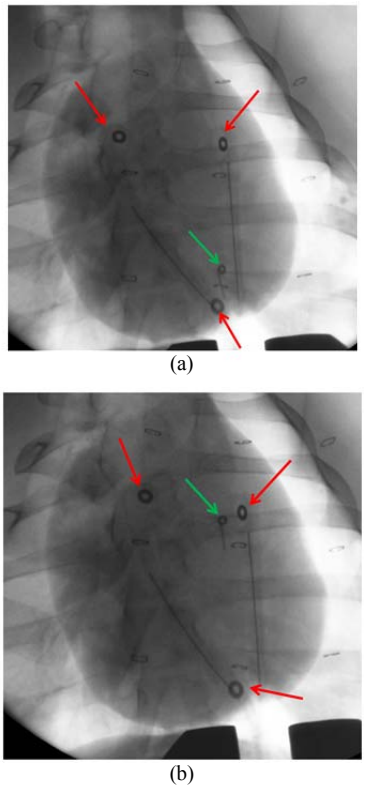

(a) (b)

Fig. 6. Two fluoroscopic views of the manipulator deployed in a porcine model in vivo, with washers affixed to the three suction chambers and the end-effector head for radiopacity. Red arrows show suction chambers, green shows the injection head. (a) The end-effector near the main base (bottom of the "V"). (b) The end-effector near the right base (right tip of the "V").

hinder their suction. The pericardium actually helps fix this problem, by applying a reactive force onto the device and allowing static equilibrium.

With the device suctioned on the anterior surface of the heart, geometric homing was done using the electronic control system. The tool was moved to each base and viewed under fluoroscope to ensure the correct position. Using the computer, the device was then moved to each base and injections were performed. A sternotomy revealed the device deployed under the pericardium and movement was done to ensure electronic control was achieved. Inspection of the device and surface of the heart showed that there was no obstruction of the suction heads due to aspiration of liquid or debris. Upon excision of the heart, two injections were found.

*2) Tool Head Motion*

Fluoroscopy was used to visualize the device during operation. Small stainless steel washers were embedded in each suction base, as well as the injection head, to aid in visualization. During operation the GUI was used to position the injection head at various locations in the reachable workspace. After deployment onto the heart, images and video were captured on the fluoroscope demonstrating the motion capabilities of the manipulator, as shown in Fig. 6. The injection head moved easily under the pericardium.

*3) Injections*

During each procedure, injection into the myocardium was demonstrated. Sample results are shown in Fig. . For each injection the tool head was moved to the edge of the robot workspace and a PTFE lumen with a 23 gauge needle tip was advanced through a PTFE sheath embedded in the tool head approximately 5 mm. Water-based ink (0.1 mL) was injected into the myocardium, allowing injections to be identified post-operatively.

## IV. Discussion

The epicardial wire robot manipulator successfully demonstrated insertion, deployment, tool manipulation, and injection *in vivo*. To arrive at a clinically relevant device, further work is needed in several areas.

Accommodation for an electromagnetic tracker will be designed into future prototypes, enabling registration to preoperative models and intraoperative image guidance.

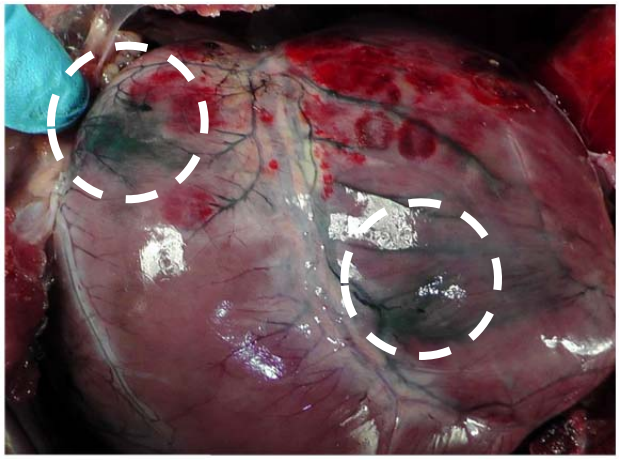

Fig. 7. Ink injections visible on the excised pig heart after operation.

Future prototypes will focus on reducing size while maintaining suction force, surgical tool movement, and injection capability. Initial prototypes have featured neoprene rubber arms for stiffness. Sheaths with thinner walls and smaller outer diameter are being considered in order to reduce the size of the bases.

The vacuum chambers can also be reduced. Initially, the chambers were generously sized in order to ensure adhesion, but new refinements will measure adhesion and scale the chambers accordingly.

Injection depth is currently manually controlled to about 5 mm. While manual injection has been relatively successful, future versions will automate injection depth to ensure consistency.

## References


[1] R. J. Hajjar, K. Zsebo, L. Deckelbaum, et al., "Design of a Phase 1/2 trial of intracoronary administration of AAV1/SERCA2a in patients with heart failure," *J. Card. Fail.*, vol. 14, no. 5, pp. 355–367, Jun. 2008.

[2] M. Jessup, B. Greenberg, D. Mancini, T. Cappola, D. F. Pauly, B. Jaski, A. Yaroshinsky, K. M. Zsebo, H. Dittrich, and R. J. Hajjar, "Calcium upregulation by Percutaneous Administration of Gene Therapy in Cardiac Disease (CUPID): a phase 2 trial of intracoronary gene therapy of sarcoplasmic reticulum Ca2+-ATPase in patients with advanced heart failure," *Circulation*, vol. 124, no. 3, pp. 304–313, Jul. 2011.

[3] M. Hedman, J. Hartikainen, and S. Ylä-Herttuala, "Progress and prospects: Hurdles to cardiovascular gene therapy trials," *Gene Ther.*, vol. 18, pp. 743–749, 2011.

[4] Y. Kawase, D. Ladage, and R. J. Hajjar, "Rescuing the failing heart by targeted gene transfer," *J. Am. Coll. Cardiol.*, vol. 57, no. 10, pp. 1169–80, Mar. 2011.

[5] J. C. Cleveland, A. L. Shroyer, A. Y. Chen, E. Peterson, and F. L. Grover, "Off-pump coronary artery bypass grafting decreases risk-adjusted mortality and morbidity," *Ann. Thorac. Surg.*, vol. 72, no. 4, pp. 1282–1288; discussion 1288–1289, Oct. 2001.

[6] M. J. Mack, "Minimally invasive and robotic surgery," *JAMA*, vol. 285, no. 5, pp. 568–572, 2001.

[7] M. J. Mack, "Minimally invasive cardiac surgery," *Surg. Endosc.*, vol. 20, no. Suppl 2, pp. S488–92, Apr. 2006.

[8] N. A. Patronik, T. Ota, M. A. Zenati, and C. N. Riviere, "A miniature mobile robot for navigation and positioning on the beating heart," *IEEE Trans. Robot.*, vol. 25, no. 5, pp. 1109–1124, Jan. 2009.

[9] J. Merlet, "Wire-driven parallel robot : open issues," *Rom. 19-Robot Des. Dyn. Control. Proc. 19th CISM-IFtomm Symp.*, vol. 544, pp. 3–10, 2013.

[10] E. J. Lehr, E. Rodriguez, and W. R. Chitwood, "Robotic cardiac surgery," *Curr. Opin. Anaesthesiol.*, vol. 24, no. 1, pp. 77–85, 2011.

[11] T. Kaneko and W. R. Chitwood, "Current readings: Status of robotic cardiac surgery," *Semin. Thorac. Cardiovasc. Surg.*, vol. 25, no. 2, pp. 165–70, Jan. 2013.

[12] J. Albus, R. Bostelman, and N. Dagalakis, "The NIST ROBOCRANE," *J. Robot. Syst.*, vol. 10, no. 5, pp. 709–724, 1993.

[13] T. Bruckmann, L. Mikelsons, T. Brandt, M. Hiller, and D. Schramm, "Wire robots part I: Kinematics, analysis & design," in *Parallel Manipulators, New Developments*, J.-H. Ryu, Ed., Vienna: InTech, 2008, pp. 109–132.

[14] R. L. Williams and P. Gallina, "Translational planar cable-direct-driven robots," *J. Intell. Robot. Syst.*, vol. 37, pp. 69–96, 2003.

[15] R. Verhoeven, M. Hiller, and S. Tadokoro, "Workspace of tendon-driven Stewart platforms : Basics, classification, details on the planar 2-DOF class," in *Proc. 4th Int. Conf. Motion and Vibration Control*, 1998, pp. 871–876.